



3D Geomodeling for Europe

Project number: GeoE.171.005

Deliverable 4.1

State of the art in uncertainty visualization

Authors and affiliation:

Björn Zehner

[BGR]

E-mail of lead author:

Bjoern.Zehner@bgr.de

Version: 21-06-2019

This report is part of a project that has received funding by the European Union's Horizon 2020 research and innovation programme under grant agreement number 731166.



Deliverable Data		
Deliverable number	D4.1	
Dissemination level	Public	
Deliverable name	Report on state of the art in uncertainty visualization	
Work package	WP4, Uncertainty in Geomodels	
Lead WP/Deliverable beneficiary	BGR	
Deliverable status		
Submitted (Author(s))	20/06/2019	Björn Zehner
Verified (WP leader)	20/06/2019	Björn Zehner
Approved (Project Leader)	21/06/2019	Stefan Knopf

GENERAL INTRODUCTION

When 3D models of the geological subsurface are built with large extents, for example on basin scale, the underlying data are usually distributed unevenly, e.g. clustering in regions with economically interesting reserves, while being very sparse elsewhere. Further the data itself can only be interpreted with a certain degree of uncertainty, and finally the whole process of generating a 3D model from the different data is subject to interpretational issues, thus generating additional uncertainty.

This uncertainty characterizing the 3D models stands in stark contrast to the way in which the 3D modelling results are usually visualized these days. The software packages that are used for 3D geological modelling, such as Skua-Gocad or Petrel, already provide visualization methods that are currently used to communicate the 3D models to the stake holders or the public. Further 3D models are published on the world wide web, using the necessary web-technology to present these models in a browser. The visualization is usually done by rendering stratigraphic interfaces and faults as triangle- or quadrangle-meshes in 3D space and it pretends that the 3D subsurface is known exactly, sometimes giving the position of a mesh's vertices with a precision of up to a millimeter. In reality, however, we often do not know if a certain fault should be moved up or down a hundred meters, if it extends hundred meters more or less, or even if it actually exists at all or has a complete different shape. How do we express the magnitude and different types of uncertainty in our 3D models and how can we estimate and handle the uncertainty? Work package 4, "Uncertainty in Geomodels" which is part of the GeoERA project 3DGEO-EU, will work towards establishing the necessary workflows to provide a visualization of the 3D models, including their uncertainty.

As usual, the first step of such a work package is to look at what has been done already and how the existing methods could be used. This report, the first WP4 deliverable (D4.1), will therefore capture the state of the art in uncertainty visualization, focusing on the computer graphics and visualization side of the issue and thus looking at how other scientific disciplines, such as medical sciences or engineering, have dealt with uncertainty visualization problems for a wide variety of data types. However, in order to show already how some of these methods could be applied to geoscientific data sets, some examples are provided, including data that demonstrate the corresponding visualization methods using open source software.



TABLE OF CONTENTS

1	INTRODUCTION	2
2	GENERAL CONCEPTS AND PREREQUISITES.....	6
2.1	Colour mapping	6
2.2	Polygon-based rendering versus volume rendering.....	7
2.3	Software for visualization	9
3	VISUALIZATION METHODS BY DATA AND UNCERTAINTY TYPE.....	11
3.1	Uncertainty on maps and sections	13
3.2	Uncertainty on points and lines.....	14
3.3	Uncertainty on surfaces.....	16
3.4	Uncertainty on cells.....	19
4	VISUALIZATION EXAMPLES.....	20
4.1	Comparison volume visualization and polygon-based visualization	20
4.2	Attribute uncertainty on maps and sections	21
4.3	Geometric uncertainty of points and lines	22
4.4	Geometric uncertainty of surfaces using polygon-based rendering	23
4.5	Geometric uncertainty of surfaces using volume rendering	23
4.6	The North Sea example	24
5	A SHORT INTRODUCTION TO PARAVIEW	25
6	REFERENCES.....	27



1 INTRODUCTION

When constructing 3D regional models of the subsurface, the geoscientist has to deal with a wide range of different types of uncertainty. As shown in Figure 1, the uncertainty should already be estimated and assessed during the acquisition and interpretation of the data which later form the basis of the 3D model. The location of markers for faults and horizons that are interpreted from borehole data is uncertain, especially when old logs from the archive have to be used, as the tools to determine the borehole path had, and still have, only a limited precision (see e.g. Wolf & Wardt, 1981). When seismic imaging is used, different sources of uncertainty are introduced in the different steps of the seismic processing sequence, especially during the time to depth conversion as often the velocity model can only be estimated with a limited precision (for an overview, see e.g. Thore et al., 2002).

During the next step, namely the geometrical modelling phase during which the 3D geological model is built, the propagation of the uncertainty that comes from the input data must be assessed and its influence on the final model estimated. Sometimes there are insufficient data available for a large area and the modeller has to provide some kind of model-based interpretation in order to fill the void space in the 3D model. So the modellers have to make a decision on which conceptual models they should apply (e.g. the deformation style? flexure or fracture?) which introduces additional uncertainty, often called conceptual uncertainty. The approach commonly used to assess all these uncertainties in the resulting 3D model is the use of Monte-Carlo Simulation (see, e.g., Wellmann & Regenauer-Lieb, 2012 or Schweizer et al., 2017). Different realizations of the 3D model are generated by first sampling into the input data. The depth of a borehole marker might, for example, be given as a Gaussian distribution function and for each realization the depth is randomly drawn from this function. Subsequently, a 3D model is generated for each set of randomly drawn data. These different models are then visualized or ideally could be summarized to be represented as one model which expresses the geology and its uncertainty (see, e.g. Wellmann & Regenauer-Lieb, 2012). When the resulting uncertain structural geological model is subsequently used for process simulation, it has to be propagated with attributes, such as permeability, which also involves uncertainty. Many methods have been developed to treat this uncertainty, especially in the oil & gas and the mining industry to optimize exploitation and minimize risk (see e.g. Pyrcz & Deutsch, 2014).

The last, but nevertheless important, step in Figure 1 is the visualization. When the 3D models generated are presented to the public and the stakeholders, they should be made aware of these uncertainties in those models. Currently the representation of the geological models as triangle- or quadrangle-meshes often pretends that the position of geological structures is known with a precision of a centimetre. It is one of the primary targets of this work package to find a good visualization which shows the uncertainty in 3D geological subsurface models and where this uncertainty is coming from. The visualization should be easy to understand and intuitive and might vary for different types of viewers, e.g. for experts and novices.

The aim of the work package “Uncertainty in Geomodels” is to structure the whole discussion on uncertainty in our 3D geological models and its quantification and visualization from the viewpoint of geological surveys. What is already there and what are the gaps? The work package will provide a knowledge base to assist in the future use of the visualization methods already



established in geosciences and also establish the basis for future cooperation with other research disciplines, such as computer graphics, to fill the gaps identified.

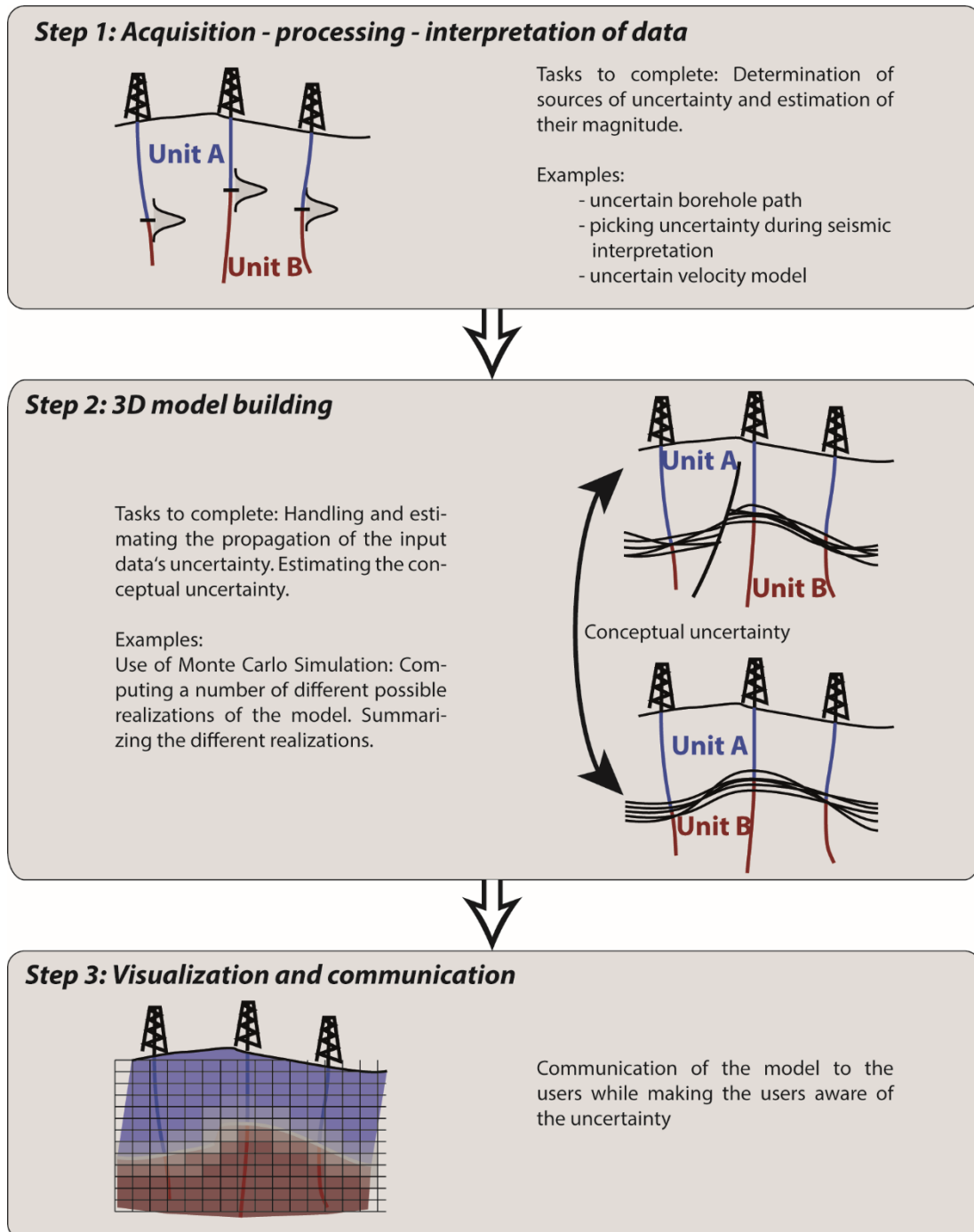


Figure 1: The different general steps to build and display a 3D geological model where the uncertainty has to be assessed.



In order to achieve this, the whole work package is structured in terms of four different tasks (see Figure 2). During the first half of the project, the aim of the first two tasks will be to establish and document the methods and concepts required. Task 1 captures the state of the art in uncertainty visualization (options for step 3 in Figure 1) and in this manner also provides information about which type of data we need to compute in order to be able to display the uncertainty in our models. It thus sheds light on where we might go and what we will need for it. Task 2 will discuss the different sources of uncertainty and the methods to propagate this uncertainty through the 3D modelling process (steps one and two in Figure 1). Task 3 and 4 in the second half of the project will apply the methods described to test different visualization options, using data sets from the pilot areas of the 3DGEO-EU project.

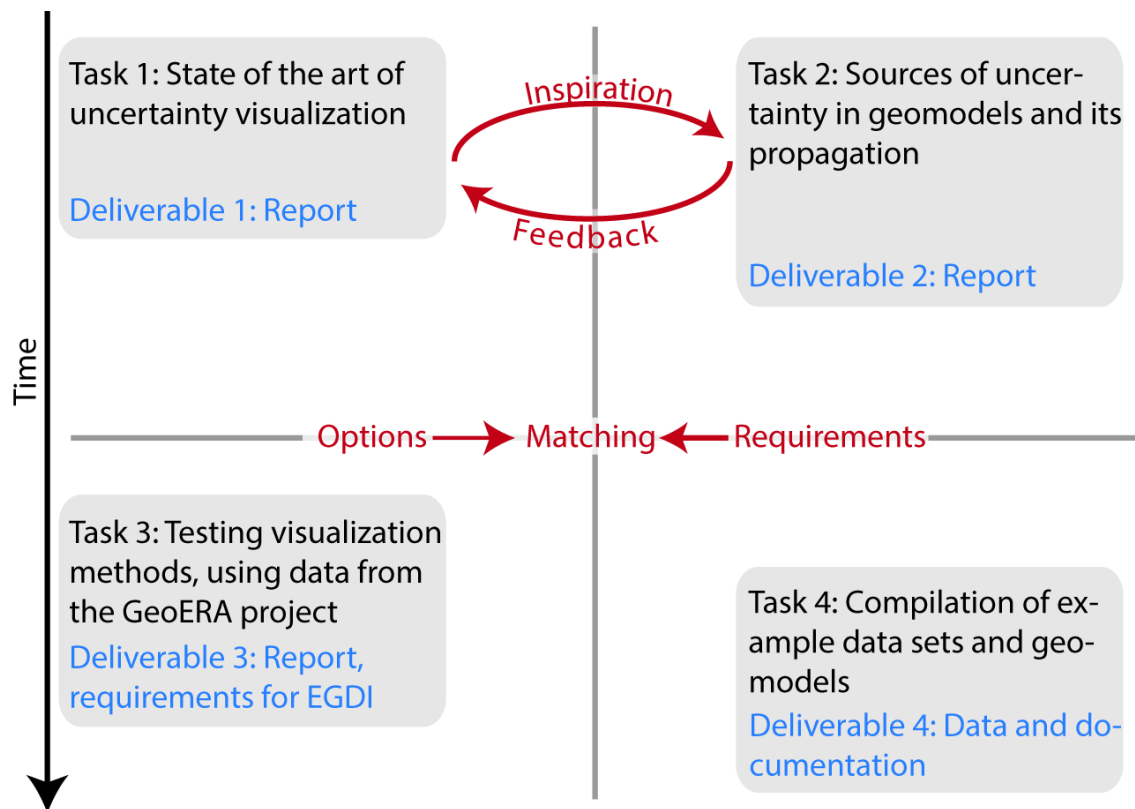


Figure 2: General structure of the 3DGEO-EU work package “Uncertainty in Geomodels”.

The overall outcome of the project will be a structured and documented overview of what is already available for the treatment and visualization of uncertainty and will thus act as a point of transfer for the necessary knowledge and skills from computer sciences to geosciences. Further it will try to suggest some best practices and workflows for how the visualization of uncertainty could be incorporated into the current standard workflows for 3D geological modelling. Finally the work package will identify what still needs to be developed and provide the necessary means, gap identification and corresponding example data sets, to give potential



outside partners, such as computer graphics groups at universities, the motivation to do research towards developing the methods lacking.

This report is the deliverable of task number one. It will capture the state of the art in uncertainty visualization and classify the different methods depending on the type of the regarded data and the type of the corresponding uncertainty (deliverable D4.1). The methods outlined have been developed by different computer graphics groups around the world - mostly for other scientific disciplines, such as for medical visualization or for the games industry. However, often they are formulated in an abstract way and could also be used for geoscientific data sets. Further, in order to enable geoscientists to make use of these methods more easily, the following will discuss how some of these methods could be made usable for geoscientists using open source software. For some data types which are commonly used in 3D geological modelling a (possibly synthetic) example data set and some kind of tutorial on how to visualize them with the open source software Paraview is made available. This work during the first stage of this task will help the project partners to gain an insight into the options they have for uncertainty visualization.

In a later stage of the project, the set of available visualization methods will be matched to the different sources of uncertainty that have been identified in Task 2 in order to identify gaps and to identify future areas of research. This match will be done based on the classification / typology of data and their specific uncertainty. As a result, two sets of requirements will be identified. The first set consists of data types and uncertainty types for which visualization methods exist already and which could be implemented as part of a 3D viewer of the information platform (EGDI). The second set consists of data and uncertainty types for which no visualization method seems to have been established so far. Here further research will be required. The user requirements, gaps and research requirements found will be documented in deliverable D4.3.



2 GENERAL CONCEPTS AND PREREQUISITES

In order to keep the discussion of the different visualization methods concise and understandable, some important general concepts in visualization should be mentioned beforehand which the reader should keep in mind when reading the document. The first one is colour mapping of different types of data at the same time, which means the application of a 2D or 3D colour map to the data (also called a 2D or 3D colour transfer function) and the understanding of different colour models. The second concept is volume rendering in contrast to the standard 3D polygon-based rendering that is most commonly used for 3D geological models.

2.1 Colour mapping

In its simplest form, the use of colour mapping is very common, for example on maps, when representing the geological units at the surface on geological maps and the heights of the terrain using colour codes. Usually either a number of bins for the data values and corresponding colour codes are defined (categorical data) or a colour map is defined as a continuously changing set of, for example, 256 or 1024 different colours and the data are mapped to these colours linearly. The colours for the maps are mostly defined and interpolated using the RGBA colour model (Red, Green, Blue and Alpha which is translucency), which is inherently the representation of the colours in most software systems as it also is the representation of colours used by monitors and on graphics boards.

However, in order to represent several types of information simultaneously, e.g. the data value itself and its uncertainty or error, more complicated techniques need to be used. Coninx et al. (2011) suggest using procedurally generated noise (Perlin noise) to scale the original data value up or down depending on its uncertainty, before they look up the corresponding colour in the colour table. In regions of high uncertainty, the visualization appears speckled while it reflects the range of the possible data values at each location.

Another option which might be simpler to implement is to do the mapping from data to colour in a different colour model first and then to convert the resulting colour into the RGB colour model. One good model for such a task is the HSV (Hue-Saturation-Value) colour model, which is explained in Figure 2. When using the standard representation as a colour wheel (top left of the Figure), one data component is mapped to Hue, which represents a colour on the circumference of the HSV colour model. A second component is mapped to the saturation, which means mapping this colour along the radius of the circle. If the second data component is at its lower threshold, it is mapped to a saturation of zero and we are at the centre of the circle (white, grey or black, dependent on Value, chosen on the linear slider on the right).

In addition to this colour mapping, shown in Figure 3, we could vary the translucency of the object in dependency of a third data component (a process often called alpha mapping). So, using alpha mapping for one component and the HSV model as a two-directional transfer function for the colour permits the representation of three different types of information. We could, for example, have a triangle-surface (horizon) that is coloured according to its data value and fades into grey where the data value is increasingly unknown and which becomes more and more translucent where it is unknown if the surface occurs at all. Unfortunately, even if the concept could easily be implemented (see Zehner et al., 2010, for an example), most of the software we use for the visualization of our data and corresponding 3D models does not supply

the flexibility required for defining such a 3D transfer function for a set of components of a data record or for multicomponent data.

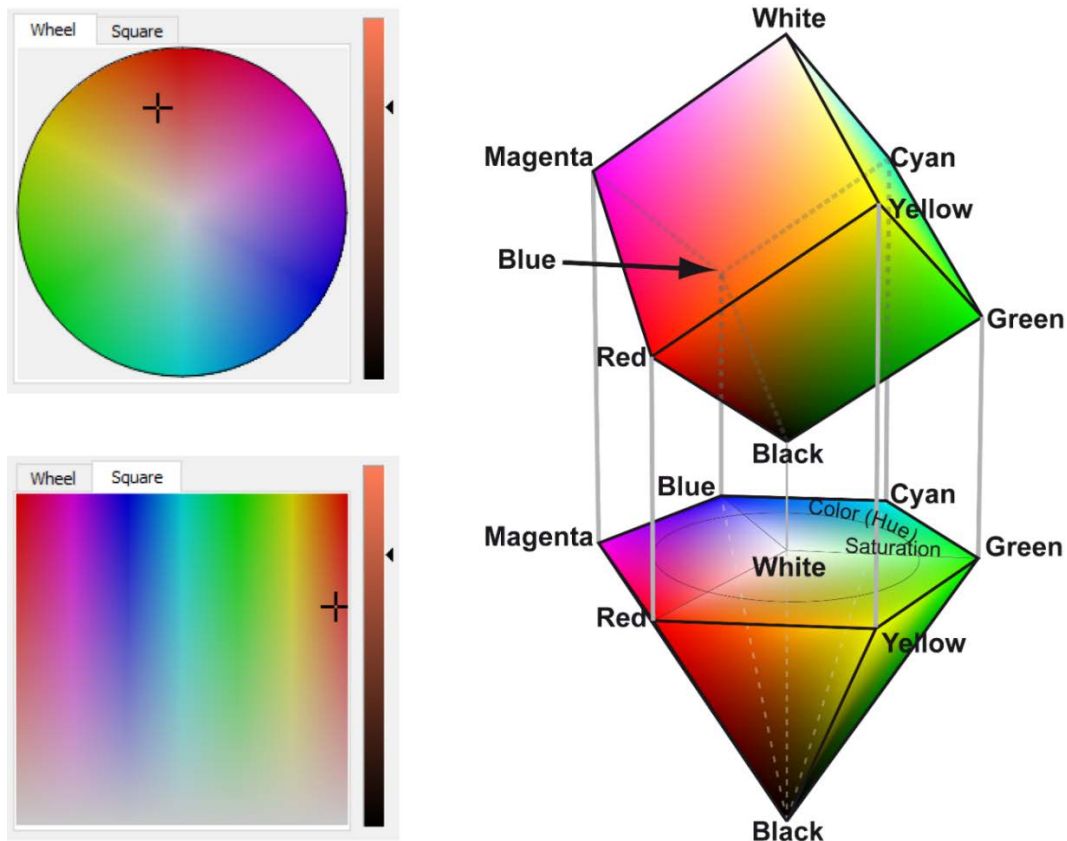


Figure 3: HSV colour model. Top left: representation as a colour wheel (screenshot from Paradigm's Skua-Gocad software). The fully saturated colours are on the circumcircle. The saturation decreases towards the centre of the circle and is zero at its centre. The centre of the circle is actually an axis with colours ranging from white (Saturation is 0 and Value is 1) to black (Saturation and Value are 0). Bottom left: Different representation of the same colour model in Skua-Gocad. The fully saturated colours from the circumcircle were rolled out from left to right while the saturation changes from top to bottom. Right: graphical representation explaining the interrelation of the RGB colour model (cube at the top) and the HSV colour model (up-side-down cone at the bottom), modified from Zehner et al. (2010). For a quantitative explanation and for pseudo-code for HSV to RGB conversion see Foley et al. (1996).

2.2 Polygon-based rendering versus volume rendering

Geological 3D models are usually rendered as a set of lines and polygons (e.g. triangles and quadrangles) which are often called geometric primitives. In a 3D structural model, the faults are represented as triangle- or quadrangle-surfaces and the geological units are depicted by rendering their interfaces (top and/or bottom) as triangle- or quadrangle-surfaces. Even if a volume is rendered, then this is usually done by showing the boundary representation (outline) as a triangle- or quadrangle-surface of the volume or, if the cell structure needs to be visible, the cells are rendered individually as their outlines (e.g. four triangles for a tetrahedral cell or 6



rectangles for a hexahedral cell). So, if a cell is assumed to be made of a semi-transparent material, it is rendered as an empty box with semi-transparent walls instead of a box which has fully transparent walls and is filled with a semi-transparent medium. Rendering is done by projecting all the polygons into screen space and subsequently scan-converting the polygons. For each pixel of the scan-converted polygons, the depth (distance to the screen) is kept, so that polygons that are nearer to the eye overwrite pixels that are further away. Semi-transparent objects must be rendered back to front (first the ones further away, then the nearer ones). The colour of the new (nearer and semi-transparent) pixel is then combined with the one that is further away.

In contrast to this rendering method, volume visualization operates on volumetric data, mostly expressed as voxel data. For each voxel the colour of the medium and the transparency is defined (or calculated on the fly via a transfer function from the voxel's data). For each pixel in screen space, a ray is shot and the absorption and reflection of the light is calculated along the beam using numerical methods and a more complicated formula. The advantage of volume visualization is that it can render semi-transparent bodies and atmospheric effects, such as fog or clouds. However, it is computationally very expensive and there is no dedicated hardware acceleration available so far. One method that is better adapted to the current graphics hardware is texture-based volume rendering. The voxel data are mapped onto sections that are cut as polygons through the data using a process called texture mapping and, if necessary, a transfer function is applied. A large number of sections are rendered back to front and each time the colour of the pixels further away is combined with new and nearer pixels, dependent on the translucency (alpha channel). Figure 4 illustrates the concept of texture-based volume rendering. For a more complete and detailed introduction on volume rendering and its different techniques see e.g. Kaufmann & Müller (2005).

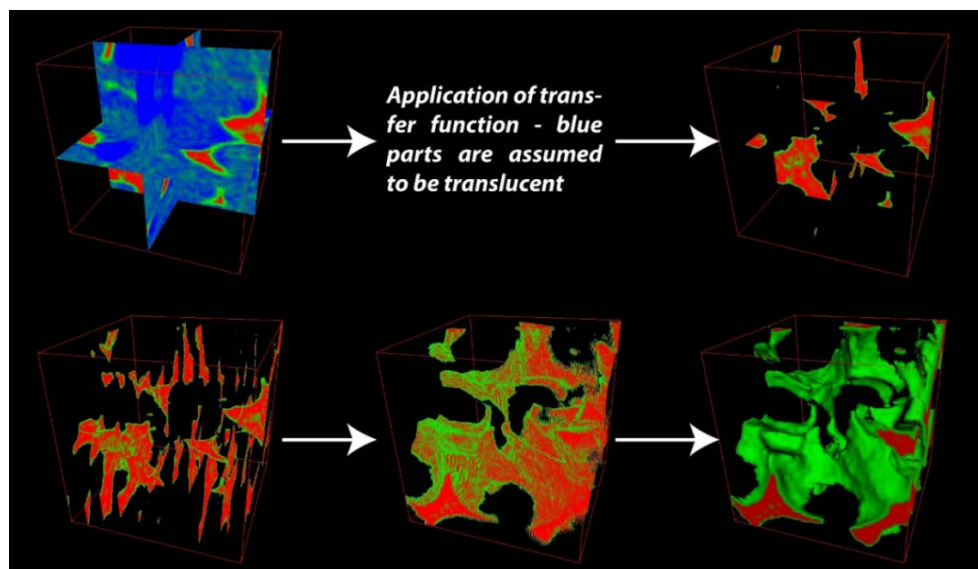


Figure 4: Concept of texture-based volume rendering, adapted from Zehner (2006). Top: data are mapped onto sections through the data set. A transfer function is applied that only renders the interesting features, leaving the rest translucent. Bottom: More and more sections extract the 3D feature, and, after applying a lighting model, the feature appears as a 3D object.



Figure 5 shows a comparison of different visualization options for a 3D geological model. The aim is, in this case, to render the model in such a way that it looks as if the different units are represented as volumes made of coloured glass (images show the example 5.1, see below).

The use of volume visualization is common in the analysis of volumetric medical data, such as computed tomography (CT) and magnetic resonance imaging (MRI). In geoscience visualization, volume rendering is currently used mainly for visualizing 3D seismic data. However, as shown in Figure 5 it might be a suitable and powerful visualization method to present 3D models of the subsurface to stakeholders in an easily understandable way. In the ideal case, the representation will look similar to a glass cube where different geological units are represented by differently coloured glass.

2.3 Software for visualization

A wide range of software packages are used by geological surveys for the generation of 3D models and all of them are also equipped to be used to visualize these models. However, firstly they can often not be easily adapted to test new visualization methods, and secondly most organizations and project partners will only work with a subset of these software packages. In order to test different visualization methods for our purposes, we need a flexible tool which allows us to do so without having to develop our own software. Gillmann et al. (2018) give an overview of different freely available software tools and evaluate them for their ability to deal with uncertain data. They distinguish the software tools according to its intended use, such as information visualization, geospatial visualization or graph visualization and according to the ability to transform the data and generate new data sets by processing the initial data. Further a number of software tools exist that were specifically tailored to certain application domains in order to explore the uncertainty in data sets interactively by using, for example, several linked views (different visual representations) of the same data. Potter et al. (2009), for example, implemented such a system for analyzing ensemble data from weather forecasting and Li et al. (2007) implemented one for astrophysical data. Prašni et al. (2010) and Saad et al. (2010) describe systems which calculate and visualize uncertainty during the segmentation (image classification and interpretation) process of volumetric medical data.

Within the data transformation category from Gillmann et al. (2018), the software Paraview is best suited to the purposes of this project. It is freely available and its flexible pipeline mechanism permits experimentation with the different visualization methods. Further the data exchange between the software Skua-Gocad and Paraview has been established by using the plugin GocadExporters for Skua-Gocad (e.g. Zehner, 2011). A short introduction on how to use Paraview and an overview of the different examples are given in the last two chapters.

Paraview supports texture-based volume rendering (within limits) and it also started to provide an interface to the ray-tracer OSPRay (Wald et al. 2017). Unfortunately Paraview does not support two-directional transfer functions, which means that the transfer function is fully controlled by one variable, which might be either the data value or the uncertainty. Thus, the methods described by Djurcilov et al. (2002), Zehner et al. (2010), and further some of the methods from Lodha et al. (1996) cannot be reproduced easily.

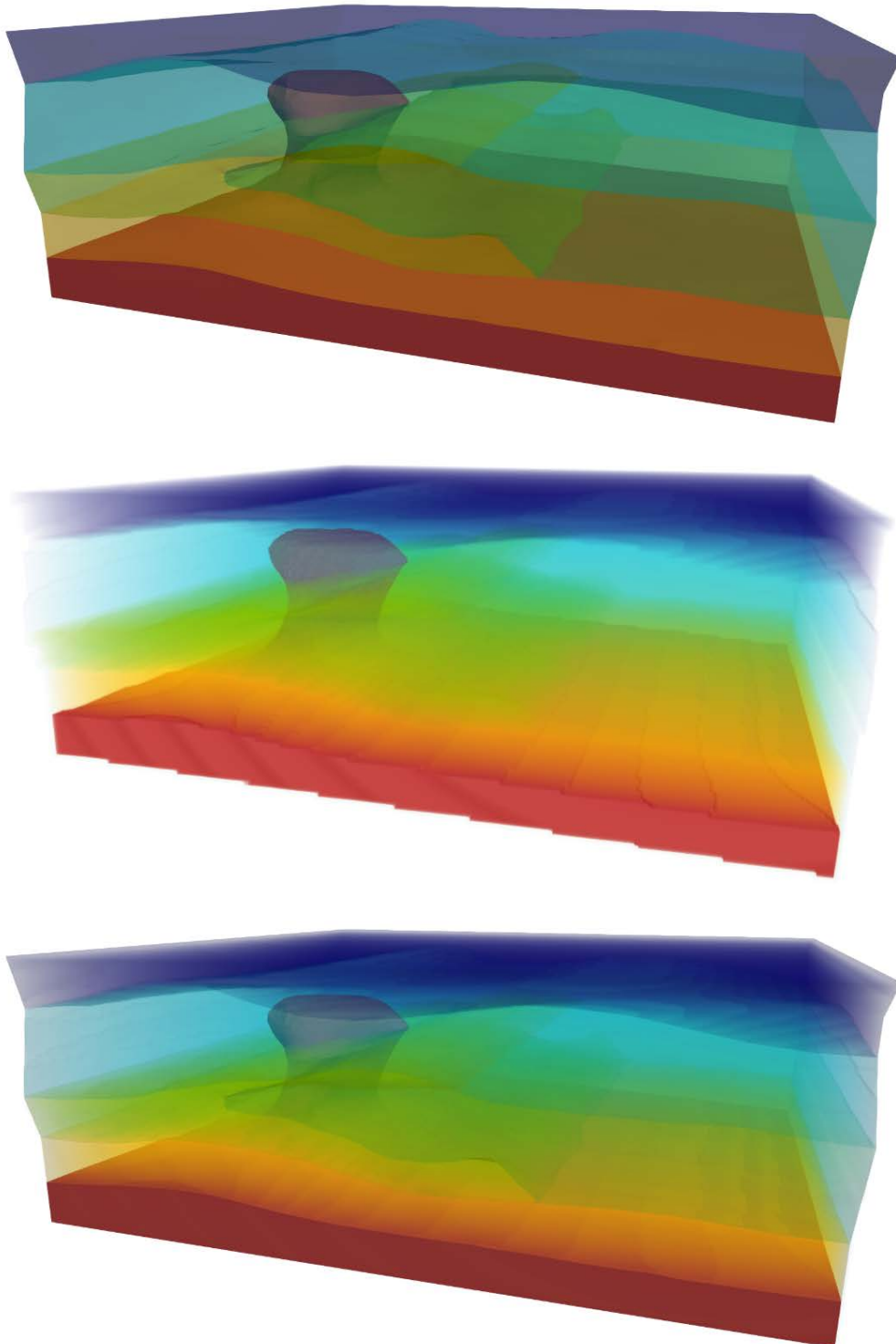


Figure 5: Three different visualization options for a volumetric 3D model. Top: Surface-based boundary representation with translucent surfaces. Middle: volume visualization. Bottom: a combination of both rendering techniques.



3 VISUALIZATION METHODS BY DATA AND UNCERTAINTY TYPE

One important classification of the different visualization methods is made according to what type of data should be visualized and what is uncertain about the data. The 3D model of the subsurface, its faults, horizons and geological units will always be represented by geometric objects, which means it will be represented by points, lines, polygons (usually triangles or quadrangles) or by cells (volumetric models) in 3D space. Further additional data can be visualized together with the geometry, such as the indication of an attribute which might be numerical scalars (e.g. physical values, such as porosity), vectors (such as a flow field), tensors (such as the permeability-, stress- or strain-tensor) or categorical data (e.g. facies or the geological unit to which a certain object or cell belongs). The necessary visualization methods for rendering and investigating these kind of data are mostly well established in the field of Scientific Visualization. Usually the geometries are rendered and the attributes are indicated by using some kind of a colour table or a set of additional objects (glyphs) for indicating vector- or tensor fields.

When uncertainty is involved, the visualization methods needed are less well established. As before, we need to establish some classification of what is uncertain in our data and develop some kind of typology for the uncertainty of the data, in order to choose later on some suitable visualization method. In this document the following types of uncertainty are distinguished.

- Geometrical uncertainty: the geometric object shown can be dislocated and deformed to a certain extent.
- Uncertain presence of objects: the geometric object, or some part of it, (possibly) does not exist at all or might have a different extent
- Uncertain attributes. For numerical scalars, the attribute would be given by some kind of a probability density function and for categorical data each category would be present at a certain location with a given likelihood. For uncertain vectors the direction and magnitude of the vector would vary and both would be given as probability density function.

The types of geometry and the types of uncertainty that are to be visualized for or on the geometry represent two dimensions of a matrix into which the different visualization methods might be shelved (see Table 1 for an example). Other dimensions can be defined. For example it might make a difference whether the visualization methods should be used by an expert user, who might be required to first receive some training to interpret the result, or if it should be understandable for a novice user ad hoc and intuitively. Further, there are some constraints on some of the methods from computer graphics, especially when the visualization of volumes is involved, with respect to the cell- or grid-types on which they work (volumetric geometries).

The papers cited in this document are, of course, only a subset of the whole literature on visualization and uncertainty and have been chosen to provide an overview. In Bonneau et al. (2014), Potter et al. (2012) and Brodlie et al. (2012) a more complete list can be found. Many of the articles cited here have been drawn from these overview articles.



Table 1: Matrix showing the different geometrical objects which are used for the visualization of 3D geological models (columns) and the different types of data with uncertainty which need to be visualized with/for these objects (rows). Some visualization methods might be very specialized and thus cover only on cell (object – uncertainty type combination) while others might be less specialized. Numbers point to the references where data of this type are treated, (0) indicates that data of this type are covered in this report in greater depth, e.g. in an example.

	Maps/Sections	Points	Lines	Polygons	Cells
Scalar attributes with uncertainty					
	(5)(6)(11)(37)(0)	(11)	(11)	(6)(11)(37)(0)	(7)(0)
Vector-attributes, uncertain direction and magnitude					
	(19)(2)(20)	(34)	(34)	(20)(34)	(16)(21)
Tensor attributes, e.g. uncertain orientation of stress / strain or permeability					
		(0)(12)	(0)(12)	(0)(12)	
Categorical attributes with uncertainty which category applies					
	(11)(0)	(11)	(11)	(11)(0)	(0, see Expl. 5.1)
Geometrical uncertainty					
	(5)(18)(22)	(0)	(0)	(17)(10)(14)(22)(28)(37)	
Uncertain presence	Fading to grey	transparency	transp.	transp.	

3.1 Uncertainty on maps and sections

Uncertain scalar fields and categorical attributes

Hengl (2003) suggests the use of the HSI (Hue – Saturation – Intensity) colour model, that is quite similar to the HSV colour model mentioned above, as a two-dimensional transfer function (colour map) for rendering numerical or categorical scalar values with uncertainty. The data values or the different categories are mapped to the hue (colour) while the uncertainty is mapped to the colour saturation and brightness. This results in a map where the data value or the different categories are shown by colour and become white or greyish when the uncertainty is high. This also means that the different colours become increasingly hard to distinguish in areas of high uncertainty. Figure 6 shows how this kind of visualization of uncertainty might look on a section. The geological units are rendered with full colour where they are known. Near to the interfaces from which the position is uncertain, they fade into grey as it becomes more and more unclear which of the units is present. The visualization shown is from the North Sea example.

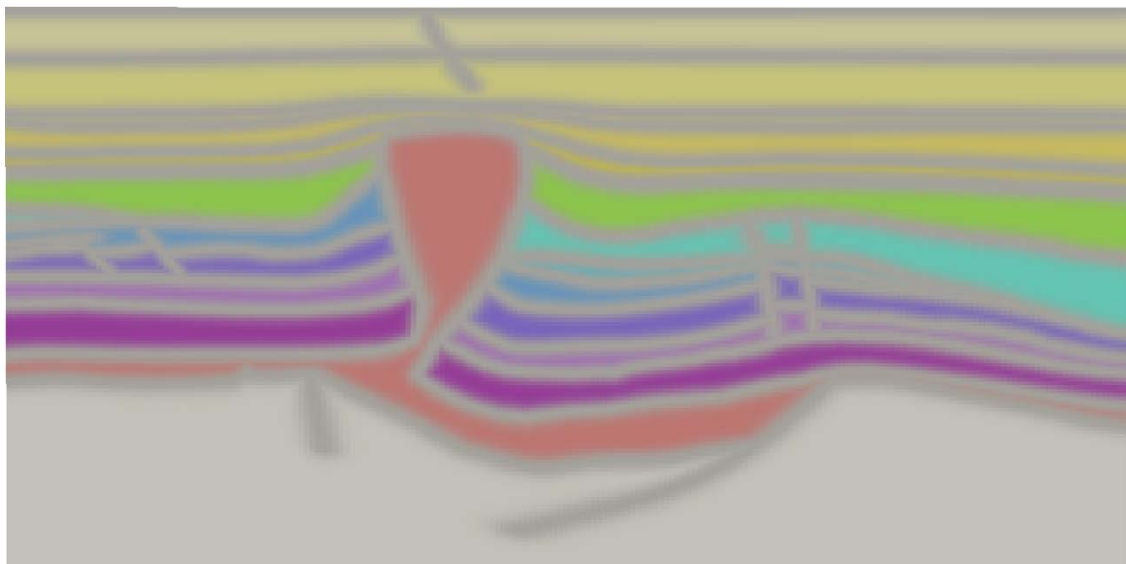


Figure 6: Visualization of a geological cross section with uncertain interfaces using a 2D colour transfer function as described in Hengl (2003) or Zehner et al. (2010). Visualization is from the North Sea example (see below) and the uncertainty has been computed for demonstration purposes and has not been assessed in reality.

Cedilnik & Rheingans (2000) suggest displaying the uncertainty by adding annotations that are deformed according to the uncertainty information and for this reason look fuzzy. For example the grid on a map that indicates latitude and longitude could be used to show in which regions the uncertainty is high by blurring the lines, or already existing annotations, such as borehole locations, fault locations or contour lines, could be used to show either their intrinsic uncertainty or the one of the underlying data display by blurring the annotations. The advantage in comparison to the method from Hengl (2003) would be that the original data display remains unchanged and readable, even in regions of very high uncertainty. The disadvantage would be that the uncertainty remains invisible in the regions between the annotations.



Osorio & Brodlié (2008) describe how the concept of contouring could be extended and thus be used for a map showing an uncertain variable on a raster image, e.g. an uncertain height field. They introduce a way to calculate “thick” contour lines depending on data value, standard deviation and required confidence, and experiment with different rendering options to show them as fuzzy contours, colour transition areas or areas where the colour appears noisy.

Further, e.g. in the geostatistics domain, different realizations of facies models (categorical data) are often rendered using side-by-side views (see e.g. Pyrcz & Deutsch, 2014 or Remy et al., 2009).

Uncertain vector fields

Wittenbrink et al. (1996) describe the use of arrow-shaped glyphs to render a vector field with uncertainty. The width of the arrowhead indicates the uncertainty in the bearing and the magnitude is either expressed by the length of the arrow or by its area. The uncertainty in the magnitude is expressed as a supplementary outline of the arrow head.

Osorio and Brodlié (2009) use an image-based technique, called Line Integral Convolution (LIC, Cabral & Leedom, 1991) to render a vector field on a map. The result could, for example, be rendered as raster data set in a geographic information system. In order to give the user a notion of uncertainty of the vector field of an attribute, such as magnitude of the vector, they suggest blurring the image in areas of uncertainty, to overlay colour by varying the Hue in the HSV colour model depending on the uncertainty and to use fog in order to incrementally whiten out areas of high uncertainty. They also show how these methods could be combined, for example by blurring the image according to the vector field and mapping the colour to the vector magnitude.

Botchen et al. (2005) describe texture-based techniques to visualize uncertainty in time-dependent flow fields. For each time step they show the flow field by texture advection which can be imagined as injecting dye at several locations (on basis of a regular grid) into the flow field. The dye follows and visualizes the streamlines. The uncertainty is shown by cross advecting (spreading) or blurring these streamlines according to the amount of uncertainty. The display can be interpreted as being similar to the arrow glyphs in Wittenbrink et al. (1996) but visually more appealing.

The above-mentioned methods only reveal the influence of the uncertainty on the vector field topology within limits. One suggestion for how this uncertain topology could be determined and visualized is shown for uncertain stationary 2D vector fields in Otto et al. (2010). On the x-y-plane the mean vector field is shown using Line Integral Convolution (see e.g. Cabral & Leedom, 1993) and the uncertain sources, sinks, saddle points and regions of influence for source-sink combinations are shown as height fields.

3.2 Uncertainty on points and lines

Geometric uncertainty

In order to show the geometric uncertainty of points, their possible displacement could be shown by rendering the centre-point (mean) and several quantiles as semi-transparent surfaces. The same could be done for lines where a hull around the line could indicate that the line stays

within this hull with a certain confidence. Figure 7 shows, by way of example, three boreholes where the standard deviation that describes the possible dislocation is assumed to increase with the length of the borehole-path (blue). Further, at the contact of the boreholes with the horizon, borehole markers are assumed for which the location would be uncertain as well.

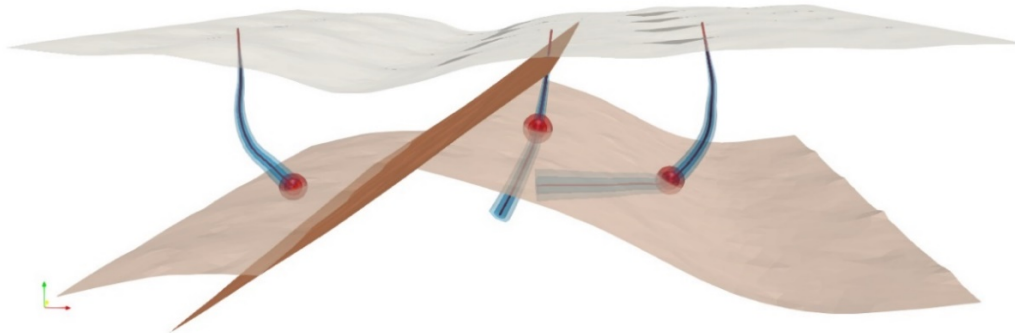


Figure 7: Visualization of points (here borehole markers) and lines (here the borehole paths) with geometric uncertainty. Visualization is from the “Uncertainty on points and lines example”, see below.

Often it can be specified that the possible displacement of a point differs depending on its direction. This can be expressed, e.g. for a normal distribution, as a 3x3 component matrix (a tensor of second rank) where the three Eigenvalues are the three standard deviations (largest, intermediate and smallest) which are normal to each other and describe a rectangular coordinate system and can, for example, be visualized as an ellipse. If the three main standard deviations are known and the transformation/rotation of the ellipse in space can be specified, the Tensor can be calculated as:

$$T = \begin{pmatrix} r_{11} & r_{12} & r_{13} \\ r_{21} & r_{22} & r_{23} \\ r_{31} & r_{32} & r_{33} \end{pmatrix} * \begin{pmatrix} stddev_max & 0 & 0 \\ 0 & stddev_med & 0 \\ 0 & 0 & stddev_min \end{pmatrix} * \begin{pmatrix} r_{11} & r_{21} & r_{31} \\ r_{12} & r_{22} & r_{32} \\ r_{13} & r_{23} & r_{33} \end{pmatrix}$$

Within the Skua-Gocad and Paraview software the 3x3 matrix must be specified as a 9 component vector (row by row). Unfortunately, within in Paraview, the tubes cannot be distorted in an anisotropic fashion. So the anisotropic uncertainty of the well path must be shown by using tensor-glyphs to indicate the uncertainty at a number of sample points along the well path. Figure 8 shows these tensor-glyphs for the wells (in blue) and the horizon markers (in red).

Uncertain scalar and vector attributes

For points and lines in space the uncertainty of scalar attributes can be rendered using colour schemes, which are equivalent to the ones described in the section on uncertainty on maps and sections (e.g. Hengl, 2003). The same holds for the glyph-based methods to render uncertain vectors which are described in Wittenbrink et al. (1996).

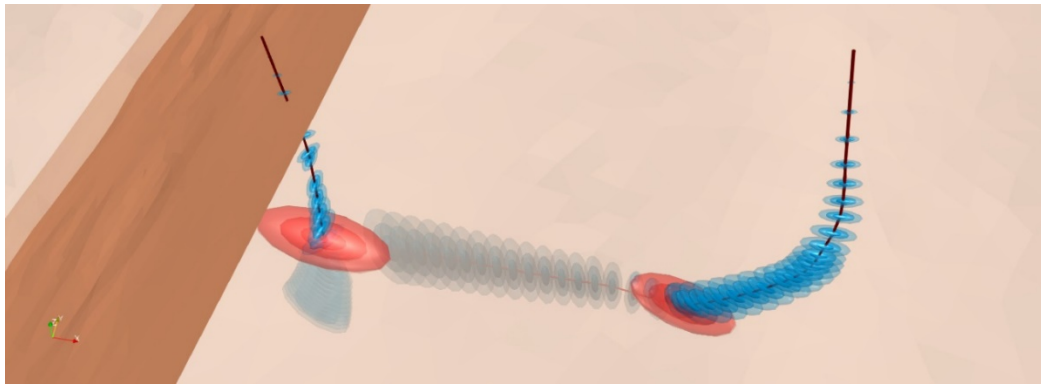


Figure 8: Visualization of points (here borehole markers) and lines (here the borehole paths) with the uncertainty of the locations described as a tensor. Visualization is from the “Uncertainty on points and lines example”, see below.

3.3 Uncertainty on surfaces

Geometrical uncertainty

Lodha et al. (1996) investigate several methods of visualizing the geometric uncertainty of surfaces regarding their location and orientation. For example they use a line or a cylinder as glyph to indicate possible displacement, a triangular glyph that spans between two vectors from the same point to indicate the range in which the surface normals can vary and spheres as volume filling glyphs between two surfaces which could indicate the envelopes that mark the confidence interval of geometric displacement. Further they map the uncertainty to visual roughness of the surface (using texture mapping techniques) and to colour and/or transparency. Figure 9 shows two different Paraview visualizations of a synthetic geoscience data set (adapted from the data used in Zehner et al. 2016) showing some of these suggested methods.

Grigoryan & Rheingans (2004) apply point-based rendering to show the positional uncertainty of a surface using a medical data set (outline of a tumor) as scenario to demonstrate their method. Instead of rendering the surface using triangles or rectangles as geometric primitive a high number of shaded points is used for each triangle. These points are displaced along the surface normal by sampling from the given distribution function that defines the uncertainty of the surface. If there is no uncertainty, this leads to the same representation as for a triangle-surface, but for regions with high uncertainty the result will be a fuzzy representation of the surface. Grigoryan & Rheingans (2004) further experiment with additional enhancements, such as using uncertainty-dependent translucency for the points or connecting the not-displaced point on the triangle-surface and the displaced point with a semi-transparent line segment, leading to a furry representation of the surface in regions of high uncertainty. Their method would be compatible with different probability distributions and the additional use of colour mapping.

Lee & Varshney (2002) extract several surfaces for molecular models that involve atoms with vibrations or otherwise uncertain positions. One surface that is rendered opaque represents the mean surface, while the other surfaces are generated for different confidence levels and lie



further outside. These surfaces are rendered with according levels of translucency and so generate some kind of glow effect for the molecular model which indicates to what extent the atoms might be displaced with a certain confidence.

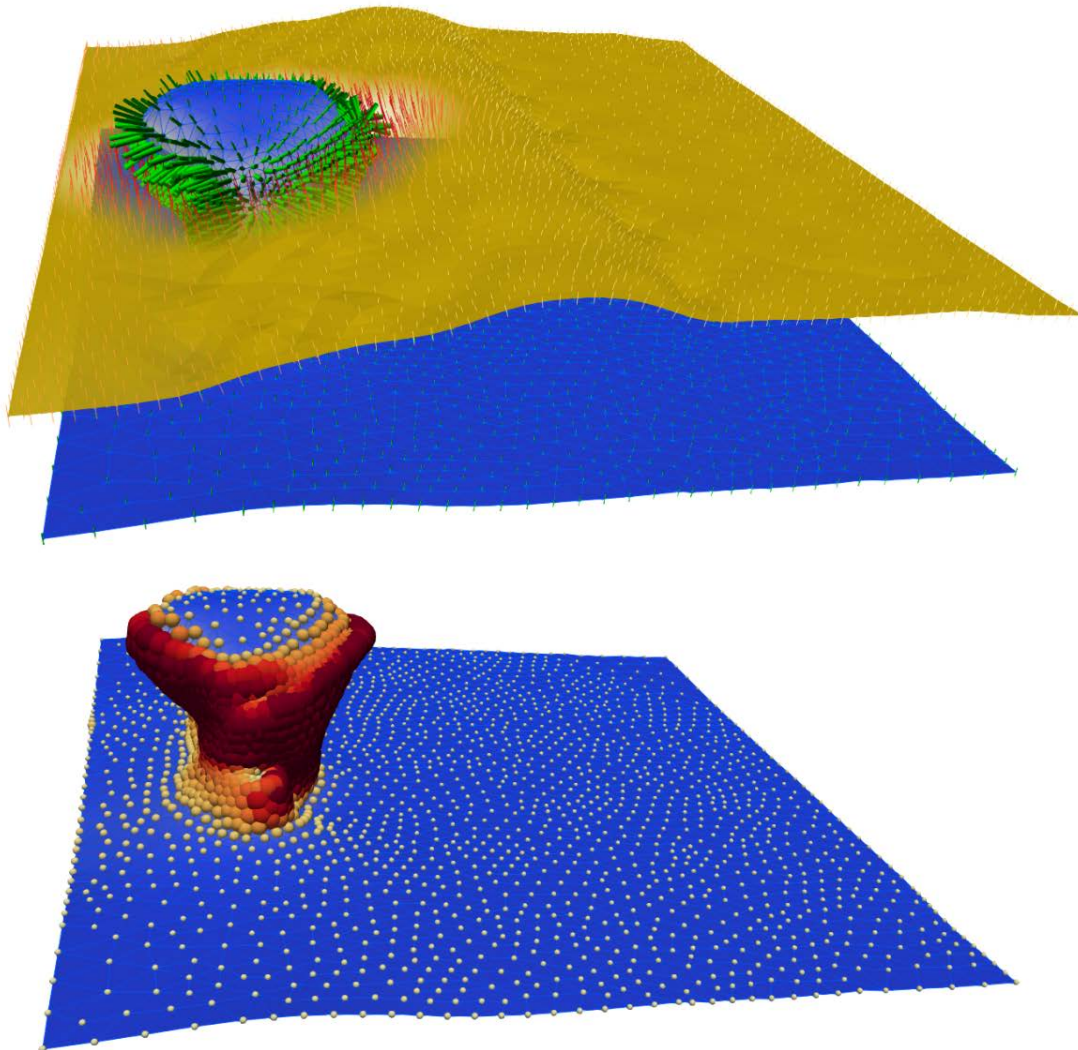


Figure 9: Examples of the visualization of geometric uncertainty on surfaces for a synthetic geoscience data set. The assumption is that the position of the boundary between the different units is less well known when it is steep or vertical, because it is often not visible in seismics in this case. Top picture: The upper horizon becomes increasingly translucent when its presence is less secure. Further the possible displacement is indicated by lines (needles). For the lower horizon (salt) the colour becomes less saturated (grey) with decreasing knowledge of its position. The possible displacement is indicated by the green cylinder. Bottom picture: The possible displacement of the horizon is indicated by the size and colouring of sphere glyphs.

We could also use volume rendering to show the uncertainty of faults or horizons by computing a volume with the distances of the cell centres to the corresponding surfaces (e.g. faults) and subsequently compute the probability that one of the surfaces (e.g. a fault) is displaced to this cell. Then applying an appropriate transfer function would lead to a visualization of uncertain faults as is shown in Figure 10. In this figure, for ease of computation, the probability depending on the distance is assumed to be the same for all faults and for each location on each fault. However, while Figure 10 shows the geometric uncertainty of the surfaces (the faults) the rendering technique used is related to techniques that show the uncertainty of scalar fields and thus is quite similar to the method described in Pöthkow and Hege (2011).

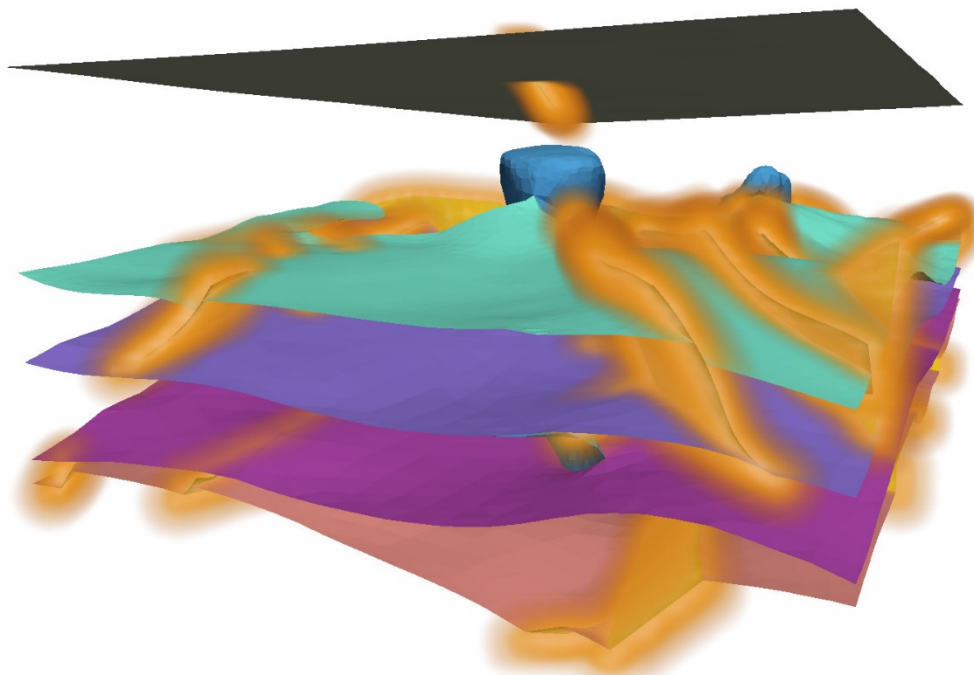


Figure 10: Visualization of uncertainty on faults, using techniques related to the method explained in Pöthkow & Hege (2011). The surfaces of the faults are assumed to be isosurfaces with the value 0 (distance field) which also are meant to represent the mean.

Uncertain scalar attributes on surfaces and categorical attributes

Uncertain scalar attributes and categorical attributes with uncertainty can be represented on a surface by a colour mapping scheme in the same way as they are represented on maps. These colour schemes could be applied independently of some of the methods described by Lodha et al. (1996) and so it is possible to show uncertain attributes on a surface with uncertain position.

Uncertain presence of a surface

The uncertainty about whether or not a surface is present at a certain location can be expressed using alpha mapping, which means that the surface is increasingly translucent, possibly vanishing when its presence is completely unclear (see, e.g., Figure 9).



3.4 Uncertainty on cells

Uncertain scalar fields

Djurcilov et al. (2002) use direct volume rendering for visualizing scalar fields, where the datum itself and its uncertainty in form of the variance are given at each point. They use a bidirectional transfer function with data values mapped to the colour and uncertainty or variance mapped to opacity. In this way they can render the certain data as a semi-transparent cloud. They further experiment with adding noise (with noise level dependent on uncertainty) and texture (with contrast dependent on uncertainty) in order to indicate the uncertainty within the volume.

Rhodes et al. (2003) extract isosurfaces from medical CT-data (using the marching cube algorithm) which is equivalent to mapping data values to opacity (with a peak for a certain value that is shown as isosurface) in the direct volume rendering equation. The uncertainty is mapped to the colour or to textures that are applied to the isosurface.

Pöthkow & Hege (2011) describe a method for rendering isosurfaces when the scalar field is given by a probability density function (PDF) or a cumulative density function (CDF) for each location. They define two functions which each depend on the iso-value that is to be extracted. The isocontour density (ICD) maps each point to probability density with respect to the given isovalue and the level-crossing probability (LCP) maps each point to probability (to assume the isovalue). As a result they generate a volume in which for each pixel the probability is defined, indicating if the isosurface crosses this cell and to which volume rendering can be applied by applying a transfer function that maps the probability value to the colour and transparency. Additionally the isosurface is extracted, using the mean values, and rendered. The result shows the isosurface and a coloured fog or glow effect that indicates the uncertainty.

Zehner et al. (2010) extract envelopes representing the confidence intervals for isosurfaces which are calculated from scalar fields given as probability density function (mean and standard deviation) for each voxel cell. The envelopes are then visualized as needles (glyphs) or as translucent surfaces. Further the HSV colour model is applied, mapping the isosurface's data value to colour and the standard deviation to a combination of saturation and value. Using this colour scheme makes the isosurfaces appear a dirty grey in areas of high uncertainty.

Uncertain vector fields

Lodha et al. (1996) visualize the uncertainty in a 3D vector field by calculating alternative realizations of the streamlines (using particle tracking) and supporting the differences between two streamlines as ribbons or by visualizing the envelopes. Their methods target more at interactively exploring regions of interest than at giving an impression of the overall vector field.

The uncertainty glyphs from Wittenbrink et al. (1996) could be adapted as 3D glyphs, such as the cones of uncertainty in Jones (2003), which are used to display the uncertainty of the first Eigenvector of a symmetric second order tensor. Further, the methods given in Botchen et al. (2005) could be adapted to be usable for 3D vector fields with uncertainty by using 3D textures and subsequently render the generated textures using volume rendering. However, in both cases the display might be cluttered if a dense information is required and so too many glyphs are rendered. Otto et al. (2011) extend their 2D approach (Otto et al, 2010) to visualize the vector field topology with uncertainty.



4 VISUALIZATION EXAMPLES

In order to demonstrate how some of the different visualization techniques could be applied to geoscience data sets by the modelling community and by the project members, we provide here several example data sets, which are, with the exception of the North Sea data set, artificial. Further the uncertainty for the North Sea data set has been created for demonstration purposes only, as the uncertainty has not been assessed quantitatively for this data set in reality.

The data sets were generated using the software Skua-Gocad and exported to an open format that is provided by the Visualization Toolkit (VTK, www.vtk.org), an open source programming library for scientific visualization. The data can be read into the software Paraview, an open source visualization software that is based on VTK (www.paraview.org). Further, Paraview allows us to create and read a state file that contains the information about which data sets are to be loaded, the visualization filter configuration and the different settings applied. Most of the pictures in this report have been generated from the example data sets and can be reproduced easily by loading these configuration files. In this way Paraview could be used as a communication tool for the project and for testing some of the visualization methods on real world data sets. A very brief introduction to where to get Paraview and how to use it to visualize the example data can be found in section 5.

4.1 Comparison volume visualization and polygon-based visualization

This example allows us to render the same structural model, a salt layer with salt dome and four stratigraphic units above this layer, using the classical way by showing the interfaces as surfaces and by indicating the different units, using volume rendering. The original data for this example are artificial and have been used in Zehner (2016).

The example data have been used to generate Figure 5 by rendering the boundary representation as transparent triangle-surfaces and filling the void space with an appropriately coloured semi-transparent medium, which could be glass, using volume rendering for the corresponding voxel data. For this visualization of a “certain” model the attribute “unit_id”, which stores a unique number that defines to which geological unit a cell or triangle belongs, is directly colour-mapped. Further, the opacity is set as a constant value for the triangle-surfaces and as a transfer function (via a table) for the voxel data.

When the actual position of the horizons is uncertain, there are two options to express this uncertainty. The first one is to render the model in the same way as the certain model (as a glass cube) but using the HSV colour model to map the uncertainty to the saturation. As shown in Figure 11, this would result in a rendering where the glass is only coloured at a location where the unit is known and becomes increasingly greyish or transparent with increasing uncertainty. As Paraview does not support 2D colour transfer functions and the HSV colour mapping, the colours have been calculated in the modelling software and have been exported to the VTK files as 4 component vectors (the attribute `rgba_uncert_sigma` ...). The first three components hold the red-green-blue (rgb) values and the fourth component holds the uncertainty which can then be used to be mapped to the opacity. In order to be able to treat the salt differently, the uncertainty of the units is mapped to the range [0.0:0.5] and for the salt to the range [0.5:1.0]. Further it has been inverted for the salt. The model is then rendered using the original colours (switching colour mapping off) while mapping the uncertainty to opacity appropriately.

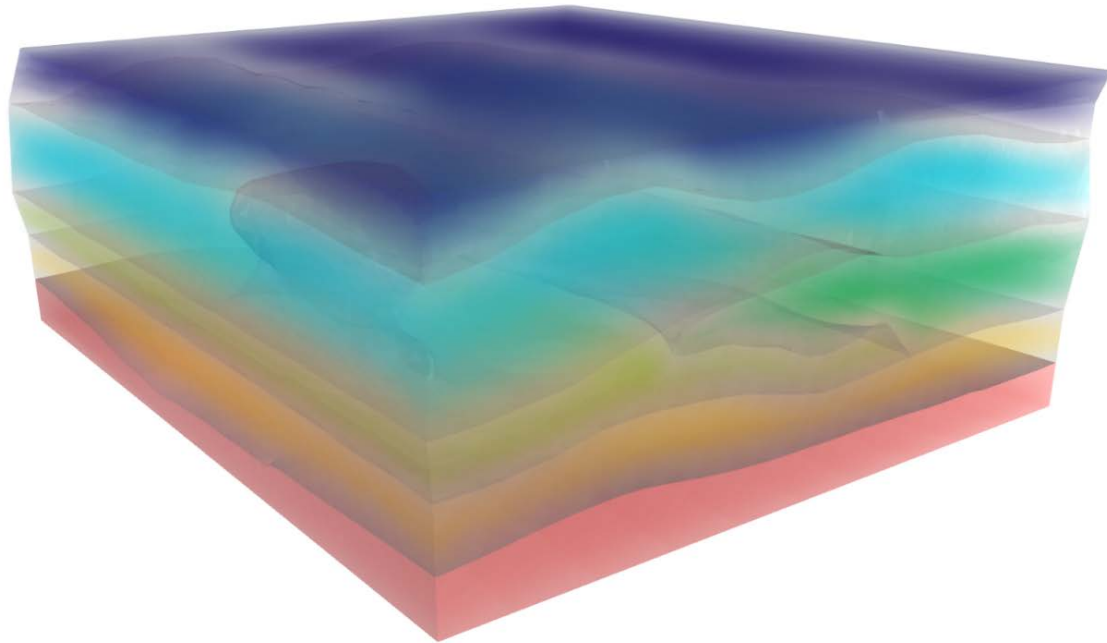


Figure 11: Volume visualization of a geological model where the positions of the geological interfaces are uncertain. The metaphor for this visualization is a glass cube where the different geological units are shown by using coloured glass and where each hue represents a different stratigraphic unit. However, near to the interfaces, the presence of a certain unit is increasingly uncertain and for this reason loses its colour, becoming transparent or milky. In order to indicate the geologist's interpretation, even in highly uncertain regions, the interfaces are rendered as grey and with high translucency. In the metaphor the interfaces could represent the reflections that would be generated when the different glass objects (units) are glued together.

The second option is to express the uncertainty in the position of the horizons by rendering them as cloudy fat surfaces. In order to do this, the attribute "rgba_uncert_sigma_300-m_fat_surfaces" of the voxel holds 4-component vectors as before, but this time the colour is fully saturated near to the horizons and fades into grey with increasing distance (which means increasing uncertainty that the horizon might assume this position).

4.2 Attribute uncertainty on maps and sections

This example shows how a bidirectional colour table could be used to represent the uncertainty on scalar attributes. The data set provided is a high-resolution voxel-model of a 10x20 km region in the German North Sea sector (see Zehner, 2018). The variable "unit_id" determines to which stratigraphic unit a voxel belongs. The uncertainty variable has been determined by a two-step process. In the first step the minimum distance for each voxel's centre to the structural interfaces (faults, horizons) has been computed, using Skua-Gocad's standard functionality. In the second step a scaled Gaussian probability density function with a standard deviation of 100m is applied in such a way, that the uncertainty is 1 for the voxels immediately adjacent to the interfaces (where the distance is zero) and fades towards 0 within the units for the voxels further away of these interfaces.



As mentioned before, Paraview does not support two-dimensional transfer functions. Further the colours for the different units often need to be set for each unit individually (for categorical data) and not by a continuously applied colour table. While, for this reason, the colours for example 4.2 have been computed in the modelling software, this example shows how the colours for the uncertain representation could be computed using Paraview's "ProgrammableFilter". Using a Python script, the colour is set depending on the "unit_id" variable, then it is blended linearly with grey in dependency of the uncertainty variable. Figure 12 shows the resulting rendering in Paraview.

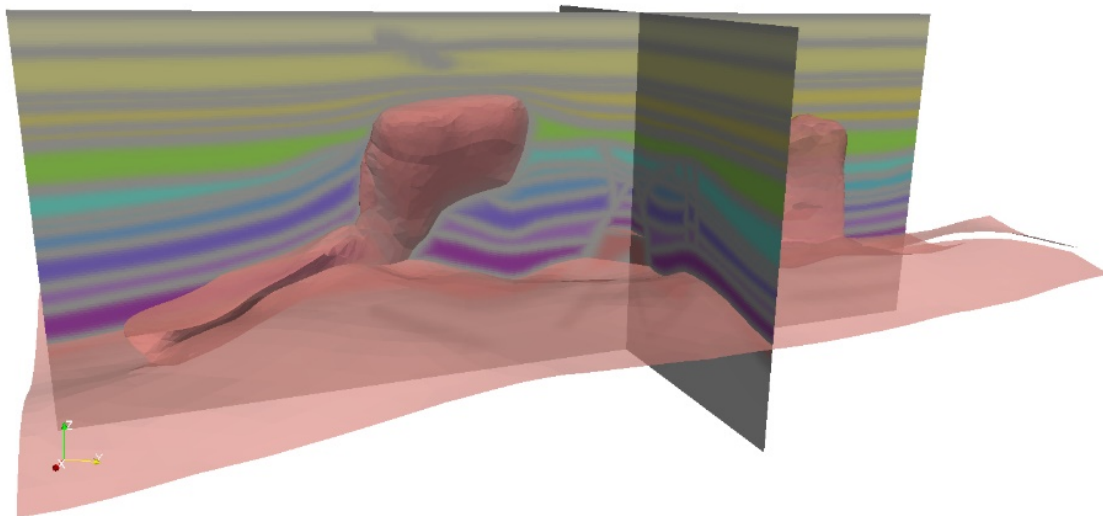


Figure 12: Visualization of two cross sections with the stratigraphic units shown by the colours. As the stratigraphic interfaces and faults of a 3D structural model can usually only be determined with a limited precision, the actual presence of a certain unit near these interfaces and faults is uncertain. This uncertainty is indicated by fading the colours into grey.

4.3 Geometric uncertainty of points and lines

This example features two surfaces which represent the ground and a horizon, and one surface which represents a fault. Further, three wells are given which carry information on the geometric uncertainty and three points which could represent horizon markers with an uncertain position. For the horizon markers and for the vertices of the well path the geometric uncertainty is given in the isotropic case as a scalar variable per vertex with the name "stddev_iso" and in the anisotropic case as a 9 component vector, named "stddev_tensor" and representing a 3x3 matrix that contains the Eigenvectors and their rotation in space. The uncertainty is visualized by varying the width of the borehole path in the isotropic case and by using glyphs along the path in the anisotropic case. The resulting visualization is shown in Figure 7 (isotropic case) and Figure 8 (anisotropic case).

4.4 Geometric uncertainty of surfaces using polygon-based rendering

The example is formed from the salt dome and one of the horizons from the synthetic model used in Zehner et al. (2016). The general assumption is that the vertical boundaries of the salt dome are less well known where they are vertical or steep. Further, the contacts of the horizons to the salt dome are often not visible in seismic images and so the reflectors become uncertain near to the salt dome. According to this assumption, two attributes have been added to each vertex. The first one is “*uncert_presence*” which is assumed to vary from 0 (we don’t know if the surface is present in this region) to one (we are sure it is present in this region because it is visible in the seismic). The second variable is “*uncert_position*” which is assumed to be something equivalent to the standard deviation, indicating for example the distance of a vertex to the 90% confidence interval (envelope) measured along the surface normal. The model has been generated and parameterized in Skua-Gocad and then exported into VTK format, using a Plugin for Skua-Gocad. After loading, the different visualization options, mostly inspired by Lodha et al. (1996) and Zehner et al. (2010) can be switched on and off. Two possible visualizations are shown above in Figure 9.

4.5 Geometric uncertainty of surfaces using volume rendering

This example shows how volume visualization could be used to visualize the uncertainty of surfaces, in this case representing faults. It has been generated from a 10x20 km pilot region in the North Sea (Zehner, 2018) which is described in more detail in the corresponding section below.

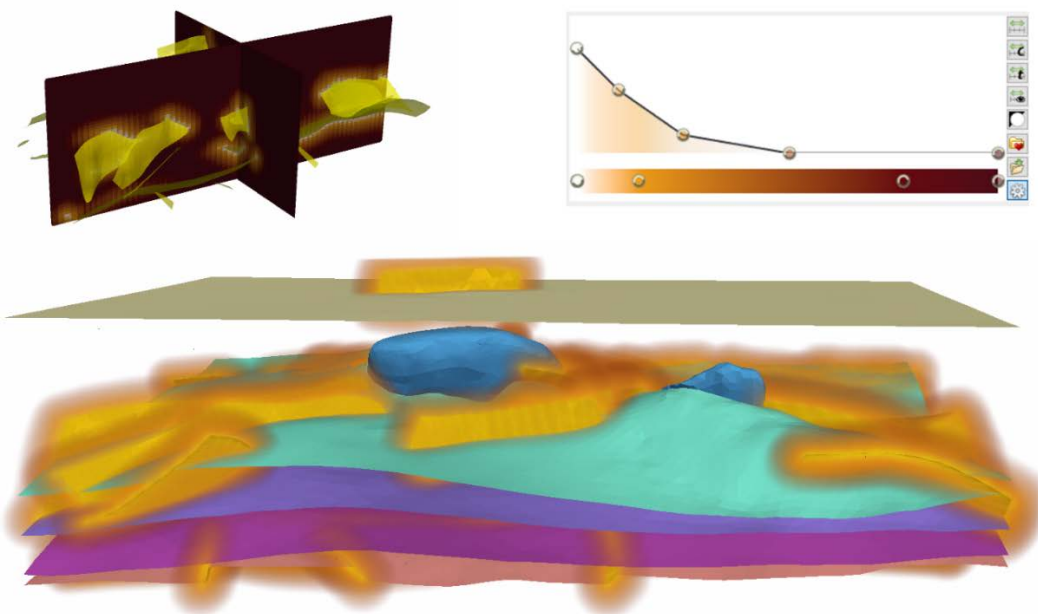


Figure 13: Visualization of faults, originally represented as triangle-surfaces, with uncertainty. Top left: the faults (yellow) and two sections through the voxel data set that is populated with the distance from each voxel to its nearest fault. This voxel data set is then volume rendered, applying the transfer function shown top right, the curve representing the alpha mapping and the colour bar the colour mapping. Bottom: The resulting visualization.



The voxel data, which are needed for the volume visualization, were generated by computing a distance field for the minimum distance from each voxel to the faults. This could be done in Skua-Gocad using standard functionality. The voxel volume is then visualized together with the triangle representation of the faults to generate some kind of glow effect to indicate that the actual position is not exactly known. While the visualization is easy to understand, it cannot be interpreted quantitatively as the viewer does not have a clear and sharp display showing in which distance the glow effect starts. Figure 13 shows a visualization of the distance field, the applied transfer function and the resulting visualization.

4.6 The North Sea example

This example shows several of the visualization techniques discussed above, using colour mapping and volume rendering. It has been generated from a 10x20 km pilot region in the German sector of the North Sea. The generation of the original volumetric model is described in Zehner (2018) and the original data are not augmented with uncertainty, which means that in reality no uncertainty analysis has been done for this model. The uncertainty has been created artificially by first creating a volume that contains for each voxel the distance to the next surface (horizon, salt interface or fault) and then applying a function that represents a scaled bell curve, so that the values for the actual position is set to one and fades to zero in 400m distance. The example shows different options for rendering the uncertainty of the horizons or the different units on the sections or as volumes and could also be applied to render volumetric models for which the information entropy, such as described in Wellmann & Regenauer-Lieb (2012), is set. Figure 14 shows the units and their uncertainties on the different sections and additionally the salt (Zechstein) as an uncertain volumetric body.

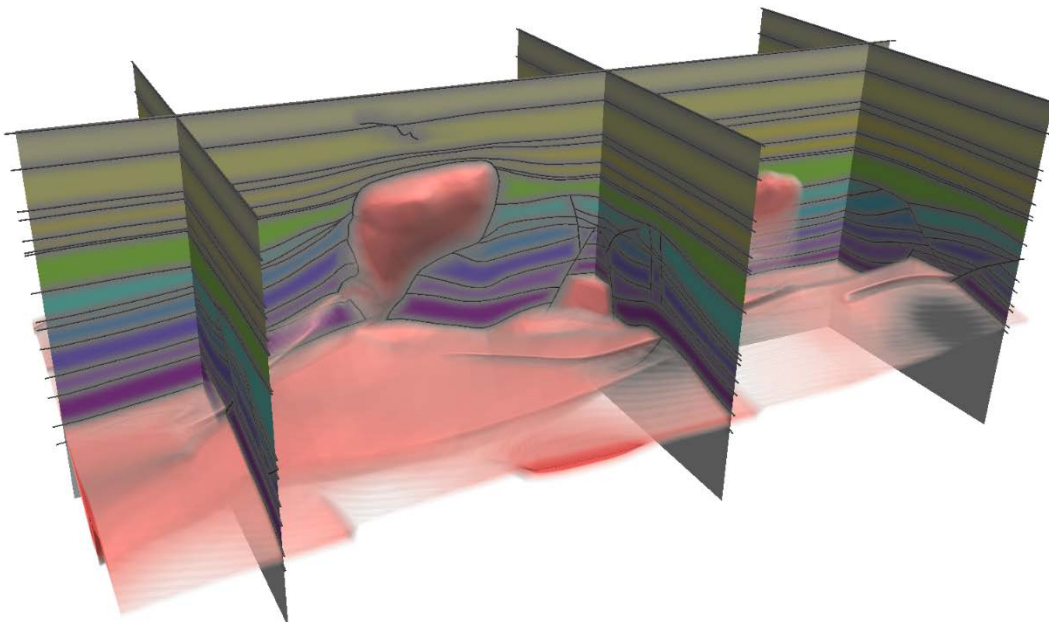


Figure 14: One of the visualizations that can be generated using the North Sea example data set. On the sections the uncertainty of the units is expressed which might be due to the fact the exact depth of the interfaces is unknown. Further the salt is shown as an uncertain volumetric body.



Figure 15 shows an example of how the visualization of sections can be mixed with the volume visualization of a sub-region and with the representation of a geological unit (the salt). However, it should be noted that mixing volume visualization with sections and other non-transparent objects can lead to rendering artefacts dependent upon the camera position. This becomes visible when rendering a high number of images from different viewpoints, e.g. for movies, and is due to the fact that rendering of the different objects is not done in an appropriate order.

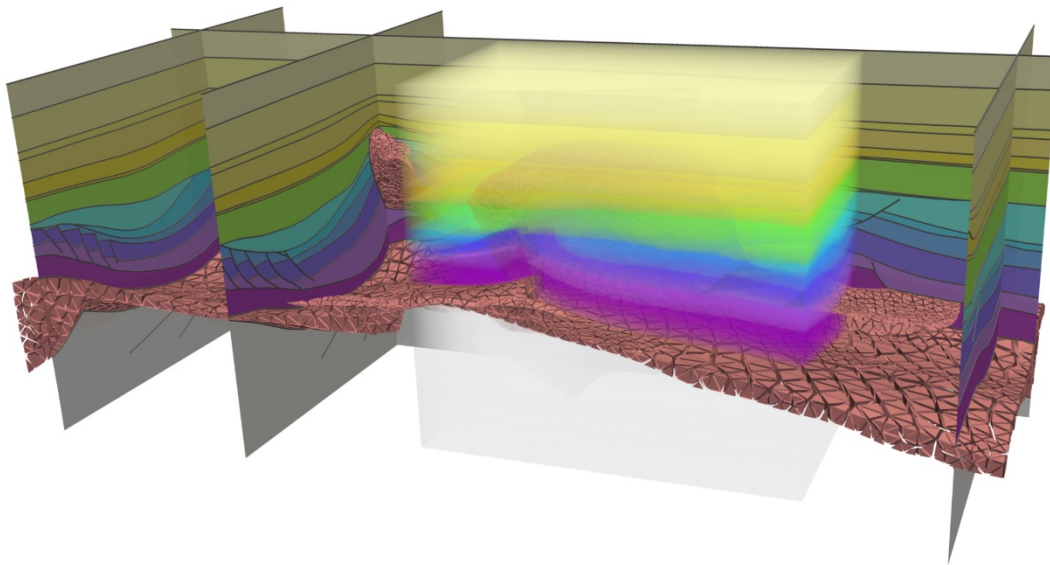


Figure 15: Certain visualization of the North Sea example, showing sections, volume visualization of a small sub-region around the salt dome and a solid visualization of the salt layer.

5 A SHORT INTRODUCTION TO PARAVIEW

The example data have been provided in VTK's file format to enable a wide range of people who are potentially interested to use the software Paraview, which is free of charge, open source and publicly available. The software can be downloaded from:

<https://www.paraview.org/download/>

We tested the example data using the version 5.5.0 and this description will be according to this version. So, for a Windows-based system, the following file should be downloaded:

ParaView-5.5.0-Qt5-Windows-64bit.zip

After installing Paraview choose "File -> Load State" and select one of the ".pvsm" files in one of the directories with the example data. A dialog "Load State Options" will open. Change the "Load State Data File Options" to "Search files under specified directory". The directory from where the data should be loaded could now be set, but Paraview will already default to the correct directory from where the state file has been loaded. So, press "ok" – Paraview will load the 3D model and display it (see picture shown in Figure 16).

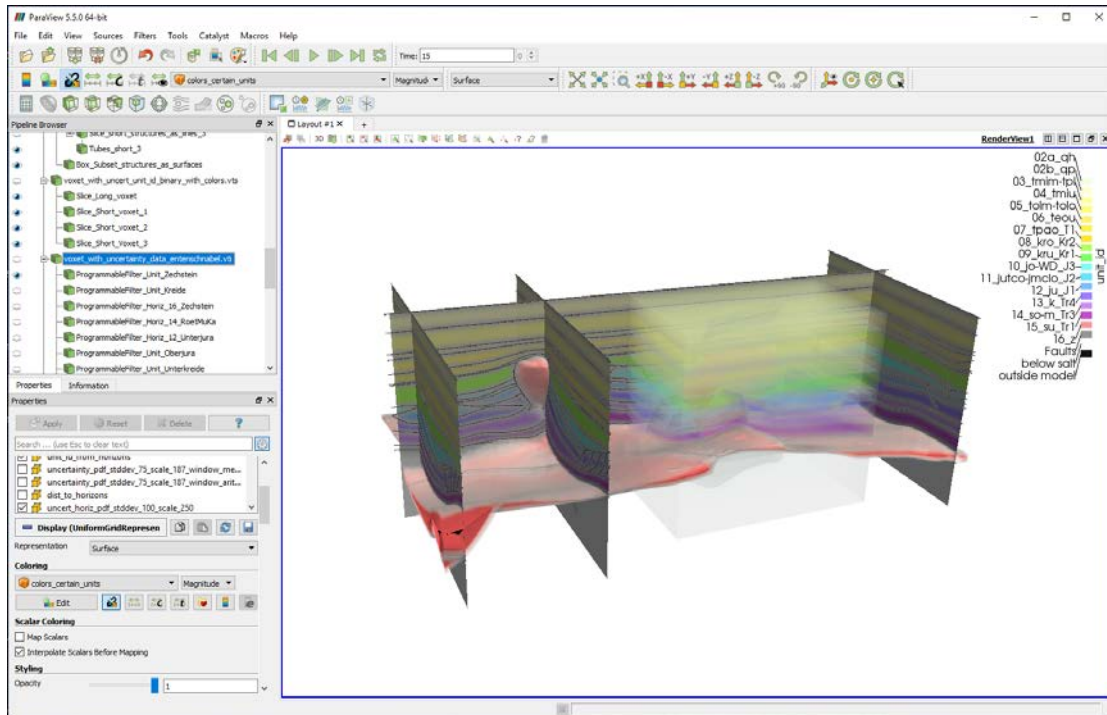


Figure 16: Screenshot of Paraview as it looks after loading the state file. To the left of the 3D window is the pipeline browser (top) and the properties panel (bottom). In the pipeline browser the visualization of the different objects can be switched on and off using the “Eye” icons to the left of the objects. When selecting a row in the pipeline browser, the properties panel switches to the view for this object and different properties can be adjusted.

Each object in Paraview either represents a data source (the file loader) which can mostly be visualized ad hoc or a processing step (a filter). The data source objects are shown in the pipeline browser with the filename as name. Further different processing steps can be applied to each object, called filters, which lead to a new representation of the object. One filter that can be applied to each of the volumetric objects is the “Slice” filter which cuts an arbitrary cross-section through the volumetric model and displays it.

When selecting one of the objects in the pipeline browser, properties can be adjusted. In the “Colouring” section of the property panel it is, for example, possible to select which of the different properties is used to colour the cells or vertices and a colour is given as an rgba vector or, if a scalar attribute should be mapped, by applying a colour table (check “map scalars”). Further, if colour mapping is applied, the colour table and opacity function can be chosen and adjusted in a dialog. This dialog is opened by checking the “Edit” button in the “Coloring” section.



6 REFERENCES

- (1) BONNEAU, G.-P., HEGE, H.-C., JOHNSON, C. R., OLIVEIRA, M. M., POTTER, K., RHEINGANS, P., SCHULTZ, T. (2014): Overview and State-of-the-Art of Uncertainty Visualization, *In: Scientific Visualization: Uncertainty, Multifield, Biomedical and Scalable Visualization, Mathematics and Visualization Series*, Springer, USA, pp.1-25.
- (2) BOTCHEN, R. P., WEISKOPF, D., ERTL, T. (2005): Texture-Based Visualization of Uncertainty in Flow Fields, *Proceedings of IEEE Visualization 2005*, Minneapolis, MN, USA, DOI: 10.1109/VISUAL.2005.1532853
- (3) BRODLIE, K., OSORIO, R. A., LOPES, A. (2012): A Review of Uncertainty in Data Visualization, *In: Dill, J., Earnshaw, R., Kasik, D., Vince, J., Wong, P. C. (Eds) – Expanding the Frontiers of Visual Analytics and Visualization*, Springer, pp. 81-109.
- (4) CABRAL, B., LEEDOM, L. (1993): Imaging vector fields using line integral convolution, *Proceedings of ACM SIGGRAPH 1993*, ACM, p. 263-272.
- (5) CEDILNIK, A., RHEINGANS, P. (2000): Procedural Annotation of Uncertain Information, *Proceedings of IEEE Visualization 2000*, IEEE, p. 77-84.
- (6) CONINX, A., BONNEAU, G.-P., DROULEZ, J., THIBAUT, G. (2011): Visualization of uncertain scalar data fields using color scales and perceptual adapted noise, *Proceedings of ACM SIGGRAPH Symposium on Applied Perception in Graphics and Visualization (PGV), Toulouse, France*, ACM, p.59-66. DOI: 10.1145/2077451.2077462
- (7) DJURCILOV, S., KIM, K., LERMUSIAUX, P., PANG, A. (2002): Visualizing scalar volumetric data with uncertainty, *Computers & Graphics*, 26 (2002), Elsevier, pp. 239-248.
- (8) FOLEY, J. D., VAM DAM, A., FEINER, S. K., HUGHES, J. F. (1969): *Computer Graphics: Principles and Practice – Second Edition in C, 1969*, Addison-Wesley, 1174p.
- (9) GILLMANN, C., WISCHGOLL, T., HAGEN, H. (2016): Uncertainty-Awareness in Open Source Visualization Solutions, *Proceedings of VIS 2016*, Baltimore, Maryland, IEEE, 4pp.
- (10) GRIGORYAN, G., RHEINGANS, P., (2004): Point-Based Probabilistic Surfaces to Show Surface Uncertainty, *IEEE Transactions on Visualization and Computer Graphics*, IEEE, pp. 564-573.
- (11) HENGL, T. (2003): Visualisation of uncertainty using the HIS colour model: computations with colours, *Proceedings of the Seventh International Conference on GeoComputation (on CD-ROM)*, Southampton, UK, 8pp, http://www.geocomputation.org/2003/Papers/Hengl_Paper.pdf
- (12) JONES, D. K. (2003): Determining and Visualizing Uncertainty in Estimates of Fiber Orientation From Diffusion Tensor MRI, *Magnetic Resonance in Medicine* 49:7-12, Wiley Interscience. DOI 10.1002/mrm.10331
- (13) KAUFMANN, A., MUELLER, K. (2005): Overview of Volume Rendering, *In: Hansen, C. D., Johnson, C. R. (eds.), Visualization Handbook*, Butterworth-Heinemann, Oxford, UK, pp.127-174. DOI: 10.1016/B978-012387582-2/50009-5
- (14) LEE, C. H., VARSHNEY, A. (2002): Representing Thermal Vibrations and Uncertainty in Molecular Surfaces, *Proceeding of SPIE on Visualization and Data Analysis 2002*, San Jose, CA, USA, SPIE.
- (15) LI, H., FU, C.-W., LI, Y., HANSON, A. J. (2007): Visualizing Large-Scale Uncertainty in Astrophysical Data, *IEEE Transactions on Visualization and Computer Graphics* 13(6), IEEE, p.1640-1647.



- (16) LODHA, S. K., PANG, A., SHEEHAN, R. E., WITTENBRINK, C. M. (1996): UFLOW: Visualizing uncertainty in fluid flow, In: Yagel, R., Nielson, G.M. (Eds), *Proceedings of IEEE Visualization 96*, IEEE, pp. 249-254.
- (17) LODHA, S. K., SHEEHAN, R. E., PANG, A., WITTENBRINK, C. M. (1996): Visualizing geometric uncertainty of surface interpolants, In: *Proceedings of the Conference on Graphics Interface 96, Toronto, Canada*, Canadian Information Processing Society, pp. 238-245.
- (18) OSORIO, R. A., BRODLIE, K. (2008): Contouring with uncertainty, In: Lim, I.S., Tang, W. (eds.), *Proceedings of the Eurographics UK Theory and Practice of Computer Graphics Conference*, The Eurographics Association. DOI: 10.2312/LocalChapterEvents/TPCG/TPCG08/059-065
- (19) OSORIO, R.S.A., BRODLIE, K.W. (2009): Uncertain Flow Visualization using LIC, *Conference Proceedings of the Theory and Practice of Computer Graphics conference 2009*, The Eurographics Association, p. 215-222, <http://dx.doi.org/10.2312/LocalChapterEvents/TPCG/TPCG09/215-222>
- (20) OTTO, M., GERMER, T., HEGE, H.-C., THEISEL, H. (2010): Uncertain 2D Vector Field Topology, *Computer Graphics Forum 29 (2)*, Wiley, pp.347-356. DOI: 10.1111/j.1467-8659.2009.01604.x
- (21) OTTO, M., GERMER, T., THEISEL, H. (2011): Uncertain Topology of 3D Vector Fields, *Proceedings of the IEEE PACIFICVIS 2011 Symposium*, IEEE, pp.67-74.
- (22) PÖTHKOW, K., HEGE, H.-C. (2011): Positional Uncertainty of Isocontours: Condition Analysis and Probabilistic Measures, *IEEE Transactions on Visualization and Computer Graphics*, vol. 17(10), IEEE, pp. 1393-1406.
- (23) POTTER, K., WILSON, A., BREMER, P.-T., WILLIAMS, D., DOUTRIAUX, C. PASCUCCI, V., JOHNSON, C. R. (2009): Ensemble-Vis: A Framework for the Statistical Visualization of Ensemble Data, In *ICDM Workshops 2009 - IEEE International Conference on Data Mining*, IEEE, pp.233-240. DOI: 10.1007/978-3-642-32677-6_15
- (24) POTTER, K., ROSEN, P., JOHNSON, C. R. (2012): From Quantification to Visualization: A taxonomy of Uncertainty Visualization Approaches, In: Dienstfrey, A. M., Boisvert, R. F. (eds.), *Uncertainty Quantification in Scientific Computing. XoCoUQ 2011. IFIP Advances in Information and Communication Technology 377*, Springer, Berlin, Heidelberg. DOI: 10.1109/ICDMW.2009.55
- (25) PRABNI, J.-S., ROPINSKI, T., HINRICHS, K. (2010): Uncertainty-Aware Guided Volume Segmentation, *IEEE Transactions on Visualization and Computer Graphics 16(6)*, IEEE, p.1358-1365. DOI: 10.1109/TVCG.2010.208
- (26) PYRCZ, M. J., DEUTSCH, C. V. (2014): *Geostatistical Reservoir Modeling – Second Edition*, Oxford University Press, 433 p.
- (27) REMY, N., BOUCHER, A., WU, J. (2009): *Applied Geostatistics with SGEMS*, Cambridge University Press, 264 p.
- (28) RHODES, P.J., LARAMEE, R.S., BERGERON, R.D., SPARR, T.M. (2003): Uncertainty visualization methods in isosurface rendering, In: Chover, M., Hagen, H., Tost, D. (Eds.), *Proceedings of Eurographics 2003 Conference, Granada, Spain*, Eurographics, pp. 83-88.
- (29) SAAD, A., MÖLLER, T., HAMARNEH, G. (2010): ProbExplorer: Uncertainty-guided Exploration and Editing of Probabilistic Medical Image Segmentation, *Computer Graphics, Forum 29(3)*, Eurographics / Wiley-Blackwell, p.1113-1122.



- (30) SCHWEIZER, D., BLUM, P., BUTSCHER, C. (2017): Uncertainty assessment in 3-D geological models of increasing complexity, *Solid Earth* 8, EGU, pp. 517-530, doi: 10.5194/se-8-515-2017
- (31) THORE, P., SHTUKA, A., LECOUR, M., AIT-ETTAJER, T., COGNOT, R. (2002): Structural uncertainties: Determination, management and applications, *Geophysics* 67 (3), pp. 840-852.
- (32) WALD, I., JOHNSON, G. P., AMSTUTZ, J., BROWNLIE, C., KNOLL, A., JEFFERS, J., GÜNTHER, J., NAVRATIL, P. (2017): OSPRay – A CPU Ray Tracing Framework for Scientific Visualization, *IEEE Transactions on Visualization and Computer Graphics*, 23 (1), IEEE, p.931-940. DOI: 10.1109/TVCG.2016.2599041
- (33) WELLMANN, J. F., REGENAUER-LIEB, K. (2012): Uncertainties have a meaning: Information entropy as a quality measure for 3-D geological models, *Tectonophysics* 526-529, Elsevier, p.207-216.
- (34) WITTENBRINK, C. M., PANG, A. T., LODHA, S. K. (1996): Glyphs for visualizing uncertainty in vector fields, *IEEE Transactions on Visualization and Computer Graphics*, Vol. 2, No. 3, IEEE, p. 266-279.
- (35) WOLF, C.J.M., WARDT, J.P. (1981): Borehole Position Uncertainty - Analysis of Measuring Methods and Derivation of Systematic Error Model, *Journal of Petroleum Technology* 33(12), Society of Petroleum Engineers (SPE), pp.2339-2350. DOI: <https://doi.org/10.2118/9223-PA>.
- (36) ZEHNER, B. (2006): Interactive exploration of tensor fields in geosciences using volume rendering, *Computers & Geosciences*, Vol. 32, Elsevier, p. 73-84. DOI: 10.1016/j.cageo.2005.05.008
- (37) ZEHNER, B., WATANABE, N., KOLDITZ, O. (2010): Visualization of gridded scalar data with uncertainty in geosciences, *Computers & Geosciences*, Vol. 36, Elsevier, p. 1268-1275. DOI: 10.1016/j.cageo.2010.02.010
- (38) ZEHNER, B. (2011): Constructing Geometric Models of the Subsurface for Finite Element Simulation, *Conference of the International Association of Mathematical Geosciences (IAMG 2011)*, Salzburg, Austria, 5th-9th September 2011, doi:10.5242/iamg.2011.0069, 14p.
- (39) ZEHNER, B., HELLWIG, O., LINKE, M., GÖRZ, I., BUSKE, S. (2016): Rasterizing geological models for parallel finite difference simulation using seismic simulation as an example, *Computers and Geosciences* 86 (2016), Elsevier, p. 83-91, doi:10.1016/j.cageo.2015.10.008.
- (40) ZEHNER, B. (2018): Constructing a volumetric model from a complex 3D structural pilot area in the German North Sea Sector, *Proceedings of the RING Meeting 2018*, Nancy, France, 18th-21st September 2018, p. 177-184.